HHS Public Access

Author manuscript

Science. Author manuscript; available in PMC 2020 June 06.

Published in final edited form as:

Science. 2019 December 06; 366(6470): 1251–1255. doi:10.1126/science.aaz0898.

Functional diversity of human intrinsically photosensitive retinal ganglion cells

Ludovic S. Mure[1,*], **Frans Vinberg**[2], **Anne Hanneken**[3], **Satchidananda Panda**[1,*]

[1]Salk Institute for Biological Studies, 10010 North Torrey Pines Road, La Jolla, CA 92037, USA.

[2]John A. Moran Eye Center, University of Utah, 65 Mario Capecchi Drive (S3140), Salt Lake City, UT 84132, USA.

[3]Department of Molecular Medicine, The Scripps Research Institute, 10550 North Torrey Pines Road, La Jolla, CA 92037, USA.

Abstract

Intrinsically photosensitive retinal ganglion cells (ipRGCs) are a subset of cells that participate in image-forming and non–image-forming visual responses. Although both functional and morphological subtypes of ipRGCs have been described in rodents, parallel functional subtypes have not been identified in primate or human retinas. In this study, we used a human organ donor preparation method to measure human ipRGCs' photoresponses. We discovered three functional ipRGC subtypes with distinct sensitivities and responses to light. The response of one ipRGC subtype appeared to depend on exogenous chromophore supply, and this response is conserved in both human and mouse retinas. Rods and cones also provided input to ipRGCs; however, each subtype integrated outer retina light signals in a distinct fashion.

In mammals intrinsically photosensitive retinal ganglion cells (ipRGCs) are a subset of retinal ganglion cells that express the photopigment melanopsin, which renders them intrinsically photosensitive. These cells participate in a set of light responses that include circadian entrainment, pupillary light reflex (PLR), and the modulation of sleep or alertness and mood as well as some aspects of vision (1). In rodents, six different morphological and at least three functional ipRGC types have been described (2–4). In addition to intrinsic photosensitivity, the ipRGCs also mediate rod- and cone-initiated photoresponses, which expand the range of sensitivity for ipRGCs to dim light. Melanopsin is also found in the human retina (5), where it is responsible for the suppression of nocturnal melatonin and PLR

*Corresponding author. lmure@salk.edu (L.S.M.); panda@salk.edu (S.P.).

Author contributions: L.S.M., F.V., A.H., and S.P. conceived the experiments. A.H. coordinated tissue collections and harvests. L.S.M. and F.V. carried out the experiments. L.S.M. and S.P. analyzed the data. L.S.M. and S.P. wrote the manuscript.

Competing interests: S.P. is the author of *The Circadian Code*, for which he receives author royalties.

Data and materials availability: All data that support the findings of this study are available in the supplementary materials.

SUPPLEMENTARY MATERIALS

science.sciencemag.org/content/366/6470/1251/suppl/DC1

Materials and Methods

Figs. S1 to S6

Tables S1 to S3

References (*23–42*)

(table S1). However, there is no report of previous direct assessment of ipRGC function in humans.

To assess the intrinsic photoresponses of human RGCs, we performed extracellular electrophysiological recordings of freshly harvested human retinas from five donors (three females, two males, 57.2 ± 8.8 years old; table S2). Small pieces of retina were placed on a multielectrode array, and the recording medium was supplemented with synaptic blockers to block excitatory rod and cone input to RGCs. In response to a 30-s pulse of mono-chromatic blue light (470 nm), photoresponsive cells were found in retinas from each of the five donors (Fig. 1A). Intrinsic responses to light were slow, sustained over the 30-s stimulation, and outlasted the stimulus by several seconds after the light was switched off (Fig. 1, A and B, and fig. S1A).

For each retina sample, we identified photoresponsive cells at an average density of 2.47 cells/mm^2 (fig. S1B), close to the lower range of the reported density of melanopsin-immunopositive RGCs in human retinas (from ~3 to 40 cells/mm^2) (6–9). Furthermore, intrinsic photoresponses from the retinas were reversibly inhibited by opsinamide (AA92593), a specific inhibitor of melanopsin (10) (Fig. 1, C and D), supporting the notion that the intrinsic photosensitivity is mediated by melanopsin.

Next, we tested whether human ipRGCs, like their rodent counterparts, can sustain photoresponses under prolonged illumination (11, 12). In response to a 10- or 20-min illumination, all ipRGCs responded for several minutes (fig. S1C), whereas 40 and 28% of ipRGCs sustained responses to the entire 10 or 20 min of light, respectively.

To assess human ipRGCs' sensitivity, we stimulated the retinas for 30 s at increasing irradiances and found similar profiles of sensitivity among donors (Fig. 1E). The ipRGC responses were rarely detectable at 2×10^{11} photons/cm^2 per second, and half-saturation sensitivities were recorded between 10^{12} and 10^{13} photons/cm^2 per second. Altogether, the response characteristics of human ipRGCs— low sensitivity, slow activation, sustained response during light stimulation, and delayed deactivation—were similar to those seen in the mouse (13), *Arvicanthis* (14), and nonhuman primate cells (15).

In mice, six subtypes of ipRGCs (M1 to M6) have been described on the basis of their morphologies, levels of expression of melanopsin, connectivity patterns, and photoresponses (2, 16). Response sensitivity (Fig. 1E) seemed to delineate at least two different types of human ipRGCs. Principal components analysis (PCA) of response parameters (sensitivity, latency, and duration) showed that, independent of the donor, ipRGC responses tended to cluster into two groups, which we called type 1 and type 2 ipRGCs (Fig. 2A and fig. S2, A to C).

Type 1 ipRGCs were more sensitive to light, with a half-maximal response at ~2×10^{12} photons/cm^2 per second and a sustained light response that lasted 47 ± 10.9 s after a 30 s pulse of light (2.1×10^{14} photons/cm^2 per second) was turned off (Fig. 2B and fig. S2D). Type 2 ipRGCs were less sensitive, with a half-maximal response at ~1×10^{13} photons/cm^2 per second, and response termination 23.9 ± 10.7 s after lights were turned off (Fig. 2B and fig. S2D). At lower irradiance levels, type 2 ipRGCs exhibited a longer response latency to

the test light pulse (fig. S2D). Overall, type 1 responses were recorded 50% more frequently than type 2 responses (1.6 ± 0.3 versus 1.1 ± 0.5 cell/mm^2, respectively) (fig. S2E). Altogether, the features of type 1 and type 2 ipRGCs suggest that they correspond to mouse ipRGC subtypes M1 and M2 (1) or type II and type III (3) (table S3). The type 1 ipRGCs also sustained longer responses under prolonged illumination, whereas type 2 cells were refractory after <5 min of illumination (Fig. 2C and fig. S2F).

Because some rodent ipRGCs may rely on the retinal pigment epithelium to supply the 11-*cis*-retinaldehyde (11-*cis*-retinal) melanopsin chromophore (17), we preincubated one retina sample in 11-*cis*-retinal for 1 hour before the recordings. In addition to type 1 and 2 responses, we also discovered a third type of ipRGC that clustered separately (Fig. 2, A and F, and fig. S2G). The cells exhibiting type 3 responses were distinct; they responded only to higher irradiances, but more strongly (Fig. 2, A and B, and fig. S2, C and H). Their response latencies were similar to those of types 1 and 2, but their response durations were shorter, rapidly extinguishing after light was turned off (fig. S2H). Finally, type 3 cells appeared to be more abundant than type 1 and 2 cells, with 30.9 cells/mm^2. Although type 1 and 2 ipRGCs' discharge rate was increased in response to the high-irradiance stimulations, their response sensitivity, latency, and duration overall were not affected by exogenous 11-*cis*-retinal (fig. S3).

To determine whether these type 3, 11-*cis*-retinal–dependent cells were specific to humans, we recorded photoresponses in retinas from adult retinal degeneration (*rd*) mice. These mice exhibit extensive degeneration of rod and cone photoreceptors; thus, light responses of 3-month-old *rd* mice are predom-inantly from ipRGCs (18). *rd* retinas produced trains of action potentials that were similar to responses recorded in human ipRGCs (fig. S4A). Upon supplementation with 11-*cis*-retinal, the number of responding cells increased (fig. S4, A and D). PCA revealed that, as in human retinas, 11-*cis*-retinal–dependent mouse ipRGCs formed a distinct cluster (fig. S4B). These cells displayed response characteristics that were different from those of other mouse ipRGCs, but similar to the type 3 cells we discovered in human retinas (fig. S4C).

To determine the spectral sensitivity of the human intrinsic light response, we measured the discharge rate as a function of wavelength (447, 470, 505, 530, and 560 nm) over ~4-log-unit irradiance range (~5×10^{11} to 5×10^{14} photons/cm^2 per second) (Fig. 3A and fig. S5). By calculating half-saturation values from the dose–response curves for each wavelength (Fig. 3A), we established the action spectra for each subtype (Fig. 3B). These data were fitted by A1 visual pigment nomograms (19) with peaks at 459 and 457 nm for ipRGC types 1 and 2, respectively (Fig. 3C). These responses are distinct from those of human rod, S, M, and L cone pigments (498, 420, 534, and 564 nm, respectively) but consistent with indirect measurements obtained for nocturnal melatonin suppression, pupillary reflex to light, and other melanopsin-dependent responses (table S1). Because of type 3 ipRGCs' limited range of responses, we did not fit their dose-response curves. Nevertheless, type 3 ipRGCs also appeared to be most sensitive around 470 nm (Fig. 3B).

In addition to intrinsic photosensitivity, ipRGCs also transmit rod- and cone-initiated photoresponses. To characterize rod and cone input, we compared ipRGCs' responses before

and after the application of the synaptic blockers. In the absence of synaptic blockers, a large number of RGCs responded to light with conventional on- or off-type responses. These results are consistent with previous reports of light responses in the human retina, and they demonstrate that the outer, inner, and intermediate layers of the retina were functionally preserved in our preparation (20, 21). After incubation with blockers and dark adaptation for 45 min, conventional RGCs stopped responding to subsequent light pulses, whereas ipRGC responses persisted (Fig. 4A). Comparison of ipRGC photoresponses before and after synaptic blockers revealed subtype-specific specialization in integrating outer retina responses with intrinsic photosensitivity (Fig. 4A and fig. S6A).

For all subtypes, extrinsic input to ipRGCs shortened response latency and lowered response thresholds. Latency was reduced by 58.4, 68.2, and 85.2% for types 1, 2, and 3, respectively, at 3.5×10^{12} photons/cm^2 per second (Fig. 4B, right, and fig. S6A); response thresholds were lowered such that ~90% of cells responded to the lowest irradiance (Fig. 4B, left). However, extrinsic input accounted for a significant portion of the sustained response and increased its sensitivity only for type 2 and 3 ipRGCs (Fig. 4C).

In summary, human ipRGCs can be separated into at least three subtypes on the basis of their responses to light, chromophore supply, and relationships with rods and cones (table S3). Different modes of chromophore regeneration within the different populations of ipRGCs may be linked to the heterogeneity in signal transduction mechanisms; in mice, a rhabdomeric cascade exists in M1 ipRGCs, a ciliary cascade operates in M4 cells, and both coexist in M2 cells (22).

It has long been assumed that the primary function of ipRGCs is to count photons (14). Our results both confirm and expand this role; rod- and cone-initiated extrinsic photosensitivity allows ipRGCs to respond to lower intensities of light and helps to sustain type 3 responses to very bright light. We also found that input from the outer retina to ipRGCs exceeds additive excitation. We observed several types of interactions—on, on or off activation, and on or off inhibition (Fig. 4A and fig. S6B)—suggesting that ipRGCs are able to mediate complex signal processing. Our study provides direct quantitative data on human ipRGC function, which will help in the development of light-based interventions for improving human health.

Supplementary Material

Refer to Web version on PubMed Central for supplementary material.

ACKNOWLEDGMENTS

We thank T. Nguyen at Salk facility services for a custom-built LED array for light stimulations and D. O’Keefe for manuscript editing.

Funding: This study was supported by NIH grants EY 016807, S10 RR027450, and NS066457 to S.P.; EY026651 and an unrestricted grant from RPB to the Ophthalmology Department at the University of Utah to F.V.; philanthropic foundation grants to A.H.; and Fondation Fyssen and Catharina Foundation fellowships to L.S.M.

REFERENCES AND NOTES

1. Do MTH, Yau K-W, Physiol. Rev 90, 1547–1581 (2010). [PubMed: 20959623]
2. Schmidt TM, Chen S-K, Hattar S, Trends Neurosci. 34, 572–580 (2011). [PubMed: 21816493]
3. Tu DC et al., Neuron 48, 987–999 (2005). [PubMed: 16364902]
4. Zhao X, Stafford BK, Godin AL, King WM, Wong KY, J. Physiol 592, 1619–1636 (2014). [PubMed: 24396062]
5. Provencio I et al., J. Neurosci 20, 600–605 (2000). [PubMed: 10632589]
6. Nasir-Ahmad S, Lee SCS, Martin PR, Grünert U, J. Comp. Neurol 527, 312–327 (2019). [PubMed: 28097654]
7. Liao H-W et al., J. Comp. Neurol 524, 2845–2872 (2016). [PubMed: 26972791]
8. Hannibal J, Christiansen AT, Heegaard S, Fahrenkrug J, Kiilgaard JF, J. Comp. Neurol 525, 1934–1961 (2017). [PubMed: 28160289]
9. Esquiva G, Lax P, Pérez-Santonja JJ, García-Fernández JM, Cuenca N, Front. Aging Neurosci 9, 79 (2017). [PubMed: 28420980]
10. Jones KA et al., Nat. Chem. Biol 9, 630–635 (2013). [PubMed: 23974117]
11. Wong KY, J. Neurosci 32, 11478–11485 (2012). [PubMed: 22895730]
12. Wong KY, Dunn FA, Graham DM, Berson DM, J. Physiol 582, 279–296 (2007). [PubMed: 17510182]
13. Berson DM, Dunn FA, Takao M, Science 295, 1070–1073 (2002). [PubMed: 11834835]
14. Karnas D, Hicks D, Mordel J, Pévet P, Meissl H, PLOS ONE 8, e73343 (2013). [PubMed: 23951350]
15. Dacey DM et al., Nature 433, 749–754 (2005). [PubMed: 15716953]
16. Quattrochi LE et al., J. Comp. Neurol 527, 297–311 (2019). [PubMed: 30311650]
17. Fu Y et al., Proc. Natl. Acad. Sci. U.S.A 102, 10339–10344 (2005). [PubMed: 16014418]
18. Panda S et al., Science 301, 525–527 (2003). [PubMed: 12829787]
19. Lamb TD, Vision Res. 35, 3083–3091 (1995). [PubMed: 8533344]
20. Weinstein GW, Hobson RR, Baker FH, Science 171, 1021–1022 (1971). [PubMed: 5542805]
21. Kraft TW, Schneeweis DM, Schnapf JL, J. Physiol 464, 747–765 (1993). [PubMed: 8229828]
22. Jiang Z, Yue WWS, Chen L, Sheng Y, Yau K-W, Cell 175, 652–664.e12 (2018). [PubMed: 30270038]

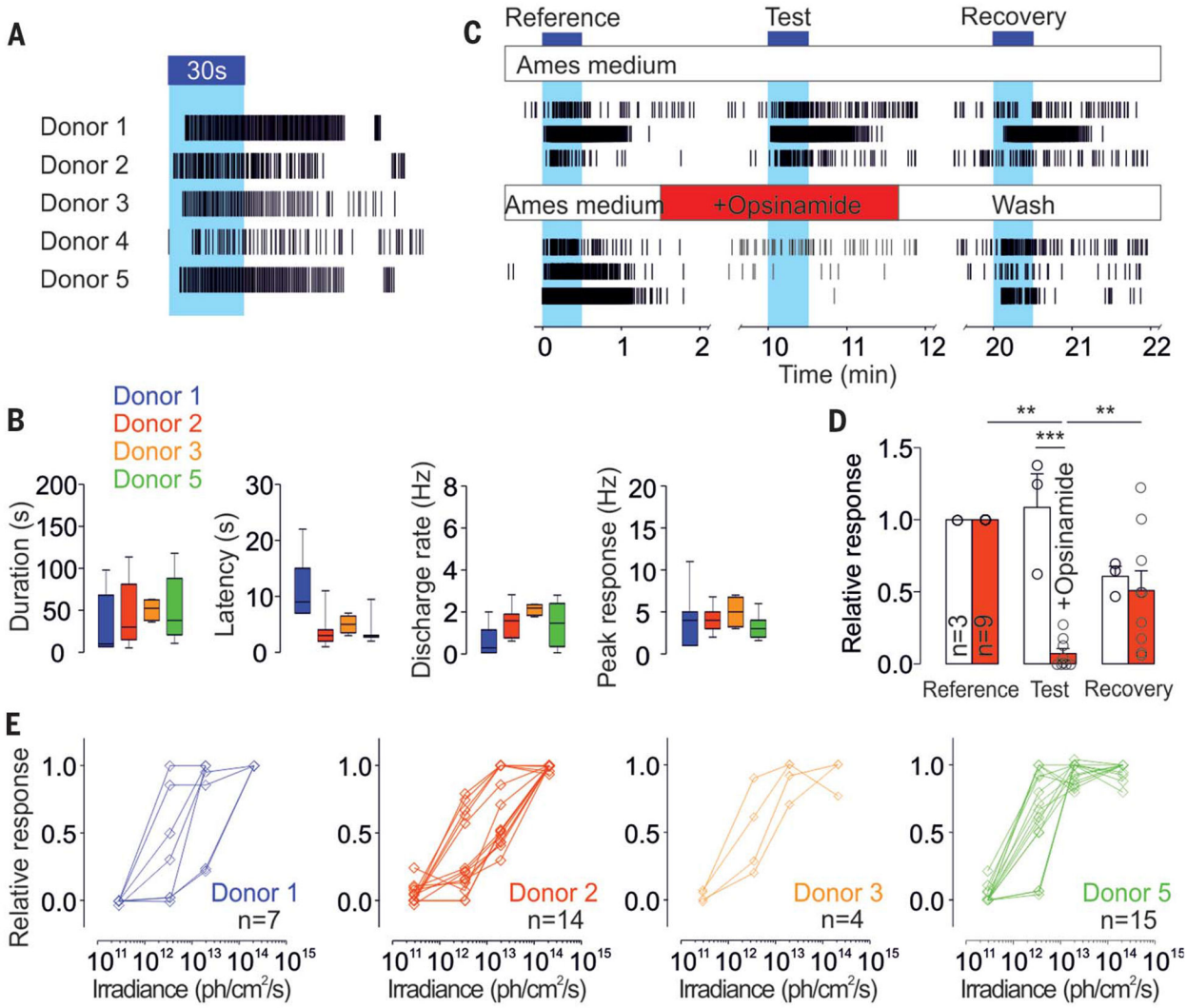

Fig. 1. A subset of human RGCs is intrinsically photosensitive.

(**A**) Representative individual ipRGC spike trains to a 30-s light pulse (~10^{13} photons/cm^2 per second, 470 nm) from five different human donors. (**B**) Average ipRGCs' response latency, duration, and amplitude in each donor (n = 7, 15, 4, and 15 for donors 1, 2, 3, and 5, respectively, where n is the number of cells). Representative individual ipRGCs spike trains (**C**) and average responses (**D**) to three identical 30-s light pulses (~10^{13} photons/cm^2 per second, 470 nm) from a control recording [n = 3; upper panel in (C), white histogram in (D)] or a recording with opsinamide (n = 9; lower panel in (C), red histogram in (D)] during the second stimulation [***P < 0.001, **P < 0.01, ANOVA (analysis of variance), Bonferroni post hoc test, one donor]. (**E**) Responses of ipRGCs stimulated for 30 s at different irradiances (from 2 × 10^{11} to 2 × 10^{14} photons/cm^{2}per second, 470 nm) in each donor (n = 7, 14, 4, and 15 for donors 1, 2, 3, and 5, respectively). ph, photons. Blue bars and blue background in (A) and (C) indicate light pulses.

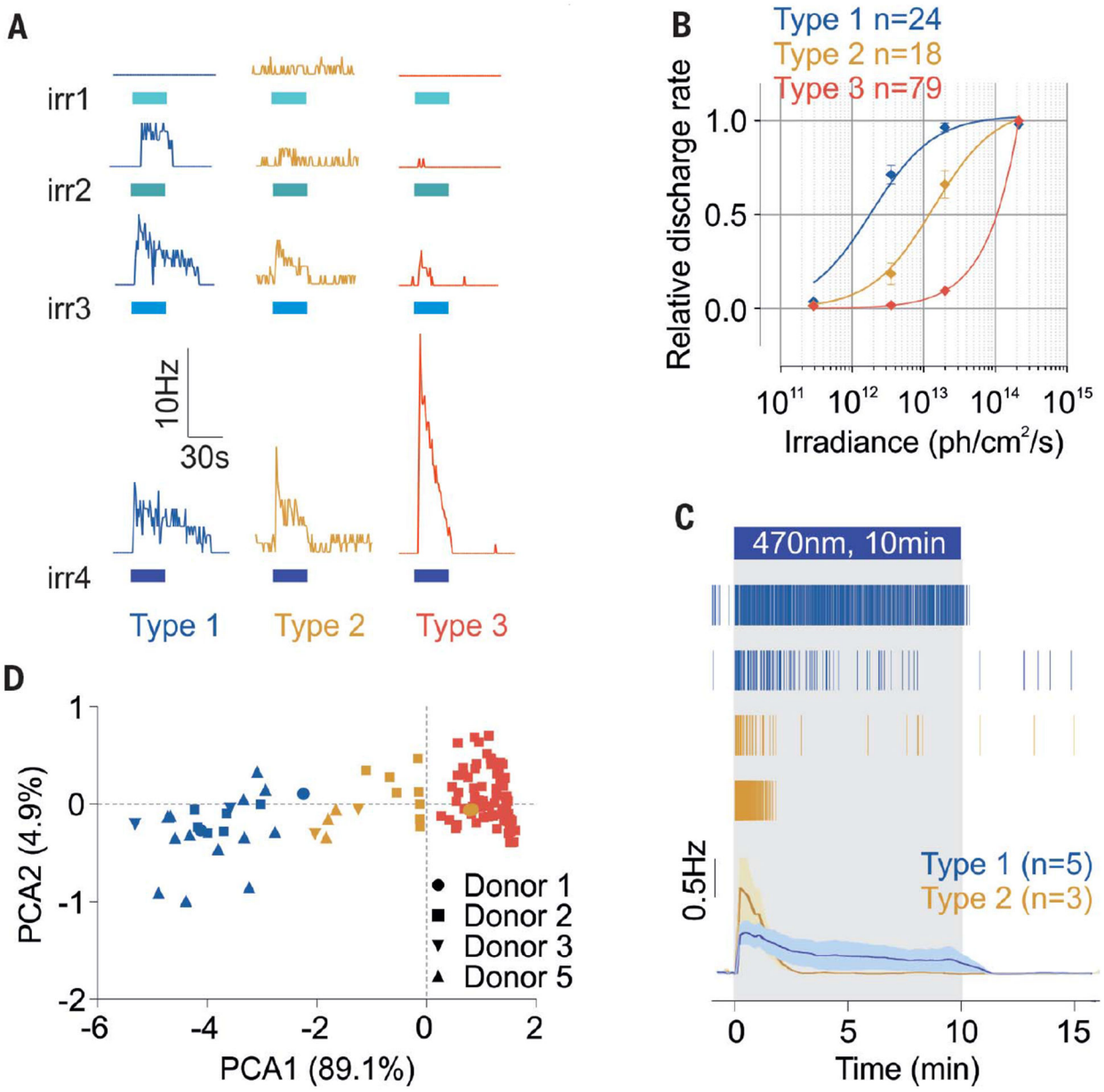

Fig. 2. Human ipRGCs display different subtypes.

(**A**) Representative responses from type 1, 2, and 3 ipRGCs to increasing irradiance light pulses [30 s, 470 nm, irradiances (irr) 1, 2, 3, and 4: 2.9×10^{11}, 3.5×10^{12}, 2×10^{13}, and 2×10^{14} photons/cm^2 per second, respectively]. Blue bars indicate light pulses. (**B**) Corresponding dose–response curves (type 1, $n = 24$, four donors; type 2, $n = 18$, four donors; type 3, $n = 79$, one donor).Error bars indicate SEM. (**C**) Representative raster plots of type 1 and 2 ipRGCs and average traces in response to 10-min light stimulations (~2×10^{13} photons/cm^2 per second, 470 nm; type 1, $n = 5$, and type 2, $n = 3$). (**D**) Principal components of the ipRGCs' response parameters (sensitivity, latency, and duration; $n = 121$, four donors).

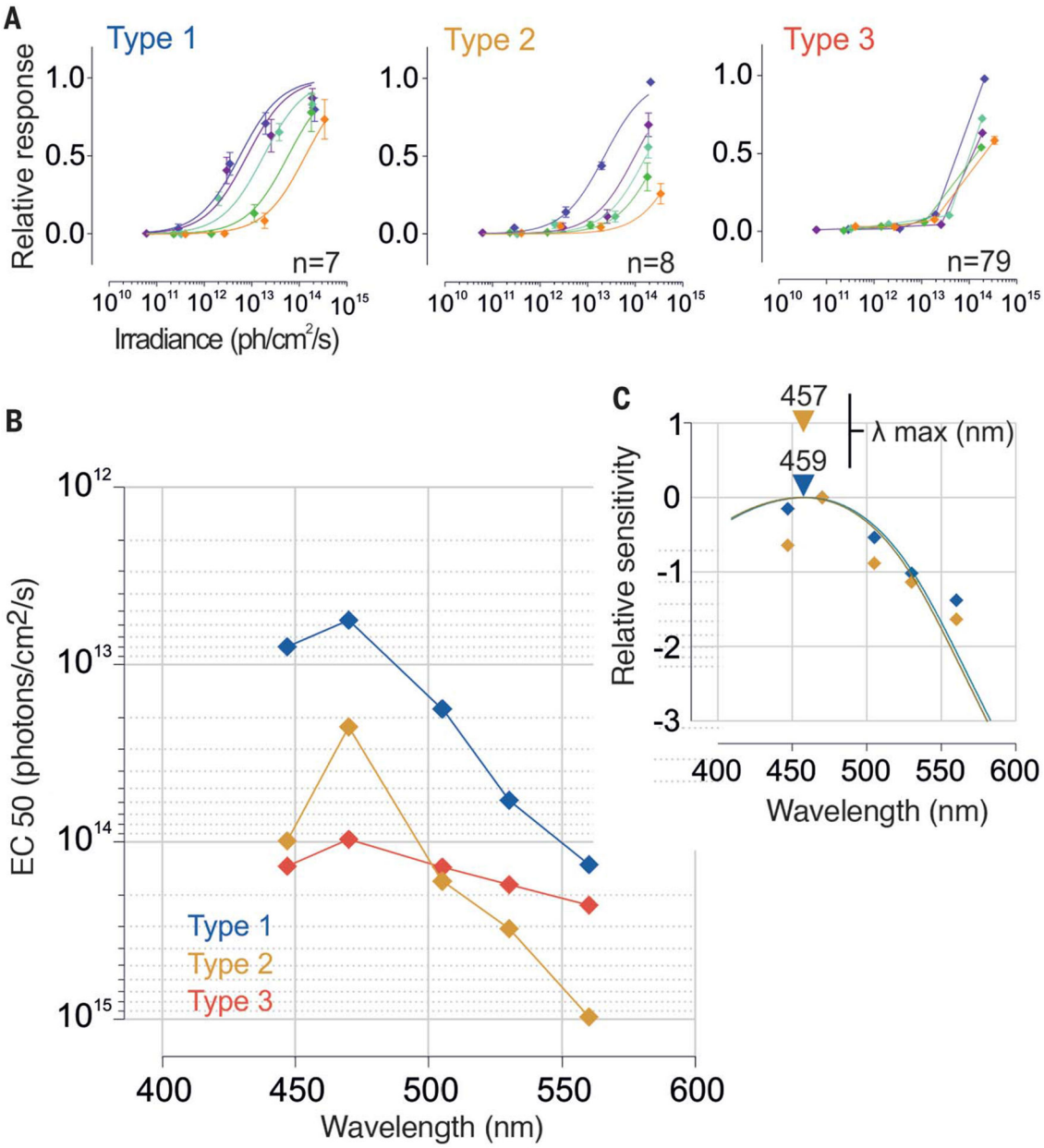

Fig. 3. Spectral sensitivity of human ipRGCs.

(**A**) Dose–response curves of each subtype to 30-s light pulses at different irradiances and wavelengths (irr1 to irr4, from 5×10^{10} to 5×10^{14} photons/cm^2 per second; 447, 470, 505, 530, and 560 nm) (type 1, $n = 7$; type 2, $n = 8$; type 3, $n = 79$; one donor). Error bars indicate SEM. (**B**) Action spectra and (**C**) best-fitted nomograms for each subtype.EC, irradiance required to drive a 50% response; λ, wavelength.

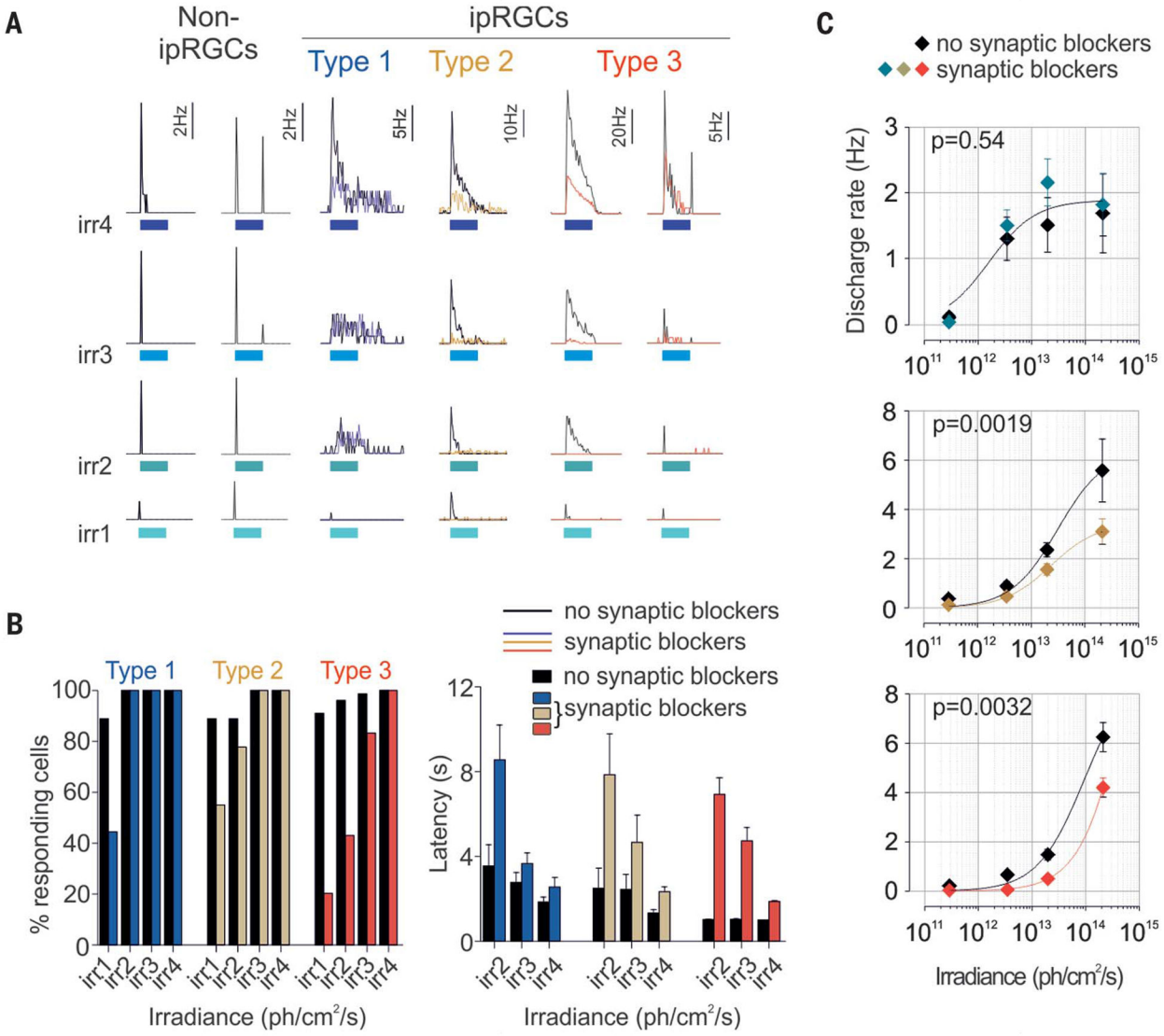

Fig. 4. Human ipRGCs integrate extrinsic signals.

(**A**) Individual examples of conventional RGCs' and type 1, 2, and 3 ipRGCs' responses to increasing irradiance light pulses before (black traces) and after (color traces) application of synaptic blockers (30 s, 470 nm; irr1, irr2, irr3, and irr4: 2.9×10^{11}, 3.5×10^{12}, 2×10^{13}, and 2×10^{14} photons/cm^2 per second, respectively). Response properties before (black bars and symbols) and after (colored bars and symbols) application of synaptic blockers are shown in (B) and (C). (**B**) Threshold and latency (effect of irradiance: type 1, $P < 0.05$; type 2, $P < 0.001$; type 3, $P < 0.001$; effect of drugs: type 1, $P < 0.01$; type 2, $P < 0.01$; type 3, $P < 0.001$; two-way ANOVAs, Bonferroni post hoc tests). (**C**) Average ipRGCs' sensitivity. In both (B) and (C): type 1, $n = 9$; type 2, $n = 9$; and type 3, $n = 78$. Error bars in (C) indicate SEM.